We are IntechOpen, the world's leading publisher of Open Access books
Built by scientists, for scientists

6,900
Open access books available

186,000
International authors and editors

200M
Downloads

Our authors are among the

154
Countries delivered to

TOP 1%
most cited scientists

12.2%
Contributors from top 500 universities

CLARIVATE ANALYTICS

BOOK CITATION INDEX

INDEXED

WEB OF SCIENCE™

Selection of our books indexed in the Book Citation Index
in Web of Science™ Core Collection (BKCI)

Interested in publishing with us?
Contact book.department@intechopen.com

Graphene-Based Material for Fabrication of Electrodes in Dye-Sensitized Solar Cells

Nguyen Huu Hieu

Abstract

Graphene-based materials have been widely studied for the fabrication of electrodes in dye-sensitized solar cells (DSSCs). The use of graphene in the cathode is to reduce the amount of platinum (Pt), which in turn is expected to reduce the production cost of DSSCs. Additionally, in the structure of cathode, graphene acts as a supporting material to reduce the particle sizes of Pt and helps to maintain the high efficiency of DSSCs. For anodes, graphene can provide a more effective electron transfer process, resulting in the improvement of efficiency of DSSCs. In this chapter, the use of graphene-based materials for fabrication of cathodes and anodes in DSSCs, including platinum/reduced graphene oxide composite (Pt/rGO) and zinc oxide/reduced graphene oxide composite (ZnO/rGO) is discussed. The fabricated DSSCs were tested using current density-voltage (J-V) curves to evaluate the efficiency. The results of efficiency demonstrate that Pt/rGO is the potential material for fabrication of cathode in DSSCs, which helps to reduce the amount of Pt and maintain the high efficiency. The efficiency values of DSSCs fabricated from ZnO/rGO anodes show that the incorporation of reduced graphene oxide in the ZnO could improve the performance of DSSCs.

Keywords: dye-sensitized solar cell, cathode, anode, graphene, zinc oxide, platinum, composite

1. Introduction

The human demand for energy has rapidly risen due to technological and economic developments. The energy problems and environmental pollutions are alarming concerns that have to be addressed urgently; therefore, researchers have explored the availability of renewable energies, such as wind energy, biomass energy, solar cells, etc. Among these types of energy, solar cells have become a potential solution to the energy shortage in terms of cost, geographical distribution, and sustainability. Since the breakthrough achievement by Grätzel and O'Regan in 1991, dye-sensitized solar cells (DSSCs) have been drawing significant attention as an alternative to fossil fuels due to the low cost, low energy consumption, simple fabrication process, and environmental friendliness [1, 2]. DSSCs are third-generation photovoltaic cells consisting of four primary components: photoanode, dye-sensitizer, electrolyte solution, and cathode.

Recently, cathodes of DSSCs are fabricated from platinum (Pt). Because Pt is a noble and expensive metal, the usage of Pt for fabrication of cathodes could lead to the increase in the production cost of DSSCs. Hence, many efforts had been made for the reduction of cathode fabrication costs to reduce the production costs of DSSCs [3].

Many research studies have been conducted for replacing Pt in cathodes by using other materials in combination with Pt. According to previous studies, copious low-cost materials were studied for fabrication of cathodes in DSSCs, such as carbonaceous materials, conductive polymers, alloys, metal oxide, transition metal-based materials including metal sulfides, metal carbides, metal nitrides, etc. [4]. Among these materials, carbon-based materials such as carbon vulcan, carbon black, activated carbon, carbon nanofibers, carbon nanotubes, and graphene have attracted more attention from researchers due to the relatively low cost, high stability, high chemical inertness, and high catalytic behavior [5]. In comparison with other carbon-based materials, graphene showed better properties, such as: having the highest electrical conductivity, fast charged carrier mobility, good chemical stability, and high surface area. These properties make graphene one of the most potential materials for fabrication of cathodes in DSSCs [6, 7]. Graphene can be synthesized from graphene oxide (GO) using the chemical reduction method, in which the synthesized graphene product is known as reduced graphene oxide (rGO). Numerous studies combined Pt and graphene for fabricating solar cells, fuel cells, and for other catalytic applications [8, 9]. In DSSCs, platinum/reduced graphene oxide (Pt/rGO) composite has been widely used for fabrication of cathode.
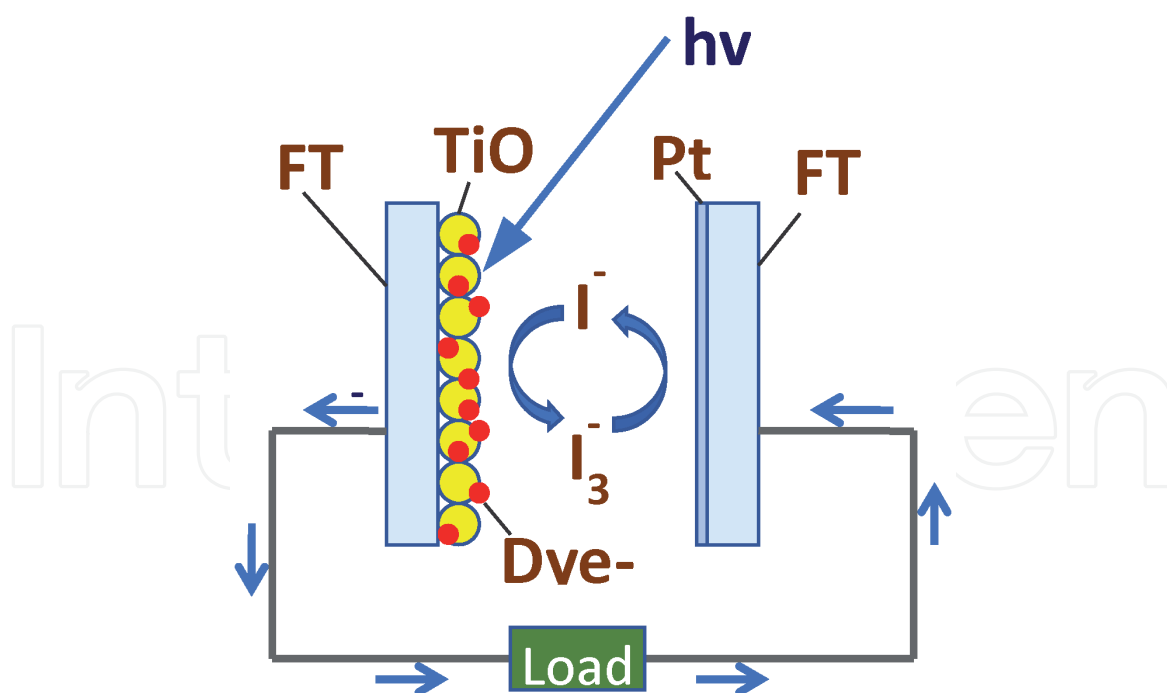
For anodes, the electron recombination processes in anode material (ZnO and TiO_2) were a phenomenon that decreased the efficiency of DSSCs. Due to the high electron mobility, lower recombination rate, electron lifetime is considerably higher in ZnO as compared to TiO_2, good transparency to visible light, high photo activity and nanocrystalline ZnO of varying morphologies, ZnO is considered as a potential material for fabrication of anodes in DSSCs. In order to increase the efficiency of ZnO-based DSSCs, graphene was studied for combination with ZnO, which could reduce the electron recombination processes of anodes. Numerous efforts have been made to investigate the performance of DSSCs fabricated from zinc oxide/reduced graphene oxide (ZnO/rGO) anodes.

In order to emphasize the potential of graphene as a promising material for fabrication of cathodes and anodes in DSSCs, this chapter is aiming to provide an overview on the current issues of DSSCs that need to be improved and the recently studied materials for fabrication of electrodes in DSSCs, especially carbonaceous materials. Subsequently, the synthesis of Pt/rGO and ZnO/rGO composite materials and the effect of synthesized materials on the performance of fabricated DSSCs are discussed. Additionally, the characterization results of Pt/rGO and ZnO which were synthesized by our group were also presented to illustrate the morphologies and structure of these materials.

2. Dye-sensitized solar cells

The structure and working principle of DSSCs are presented in **Figure 1**.

An electrode is a solid electrical conductor through which an electrical current enters or leaves an electrochemical cell or other mediums like metallic solids, liquids, gases, plasmas, or vacuums. Electrodes are usually made of good electrical conducting materials. In an electrochemical cell, an electrode is referred to as either an anode or a cathode. The anode is defined as the electrode at which electrons leave the cell and the oxidation occurs, while the cathode is defined as the electrode at

Figure 1.
Structure of DSSCs.

which electrons enter the cell and reduction occurs. For DSSCs, the anode is the light collector, thus it is also called photoanode. The anode had a deposited layer of a metal oxide semiconductor. The cathode is the electrode on which Pt and other conducting materials are deposited. The cathode in DSSCs is often called the counter electrode. In 1991, Grätzel first introduced the term "counter electrode" in his pioneering publication about dye-sensitized solar cells [10, 11].

A photoanode is typically a layer of nanocrystalline titanium dioxide (TiO_2), with a thickness of about 10 μm, coated on a transparent conductive oxide (TCO) glass substrate, such as an indium-doped tin oxide (ITO) or fluorine-doped tin oxide (FTO). Morphologies of TiO_2 materials (rod, spherical, hierarchical, and tubular) significantly affect the light-harvesting, charge injection, and charge-collecting properties of DSSCs [12, 13].

Dye-sensitizer plays a crucial role in improving light absorption within the visible region. Dye-sensitizer is described as an electron pump with inputting power from light photons. When the light irradiates the photoanode of DSSCs, electrons from the highest occupied molecular orbital (HOMO) of dye-sensitizer transfer to the lowest unoccupied molecular orbital (LUMO), then the electrons flow to the photoanode. Many types of dye-sensitizer have been used in DSSCs, such as ruthenium dyes and natural dyes. Dye N719 is a ruthenium-based dye that is used widely in DSSCs [10, 11].

After producing electrons, dye-sensitizer becomes oxidized states, and electrons need a medium to transfer back to dye-sensitizer and complete the external circuit of DSSCs. In DSSCs, electrolyte plays a role as a shuttle, which transfers electrons from cathode back to dye-sensitizer. A good electrolyte system used in DSSCs must have excellent electrical conductivity, low viscosity for easier and faster diffusion of electrons, and good interfacial contact with the nanocrystalline semiconductor of photoanode and cathode. The most popular electrolyte system used in DSSCs is iodide/triiodide (I^-/I_3^-) [10, 11].

The last main component of a DSSC is the cathode. A typical cathode of DSSCs is thin Pt layer coated on the TCO (typically FTO). At the interface between the Pt layer and the electrolyte, a reduction reaction of electrolyte occurs. This

phenomenon happens when electrons move from external loads to the cathode of DSSCs. The Pt film has three main roles in a DSSC: a catalyst for redox reaction of electrolyte, an electrolyte regenerator, and a conducting material [10, 11].

The working principle of DSSCs is different from that of conventional silicon-based solar cells. In silicon-based solar cells, the semiconductor p-n junction carried out many processes, both absorbing light and sending out current. In DSSCs, those tasks are separate. The main role of the semiconductor is to transfer electron from dye-sensitizer to FTO glass, whereas electron suppliers are the dye-sensitizer [10, 11].

The light illuminates the photoanode of the DSSCs then dye-sensitizer will absorb appropriate wavelengths and turn into excited states S*. In excited states, the dye releases electrons that will diffuse into the conduction band of semiconductor TiO$_2$ and reach FTO glass. The exciting state of sensitizers is shown in Eq. (1).

$$hv + S \rightarrow S* + e \qquad (1)$$

After that, electrons move to external loads and get back to the DSSCs at the cathode. Dye-sensitizer molecules turn into oxidized states S$^+$ after providing electron. Subsequently, those molecules are reduced by I$^-$ in the electrolyte to restore to initial states and electrolyte changes from the oxidized state I$^-$ to the reduced state I$_3^-$ as a result of reduction reactions of dye-sensitizers, as shown in Eq. (2).

$$3I^- + 2S^+ \rightarrow I_3^- + 2S \qquad (2)$$

At the cathode, the reduced state I$_3^-$ receives electrons coming back to the DSSCs from the external load and restores to I$^-$. Redox mediators move back and forth between cathode and anode mainly relying on the diffusion process. The process is shown in Eq. (3).

$$I_3^- + 2e \rightarrow 3I^- \qquad (3)$$

The above processes take place when DSSCs are illuminated continuously. Then a current is generated and flow in the external load. However, electrons in the conduction band of TiO$_2$ may follow three other routes to join in recombination reactions, as shown in Eqs. (4)–(6).

$$e_{TiO_2} + S^+ \rightarrow S \qquad (4)$$

$$e_{TiO_2} + I_3^- \rightarrow 3I^- \qquad (5)$$

$$e_{SnO_2} + I_3^- \rightarrow 3I^- \qquad (6)$$

Eq. (6) takes place on the interface between FTO and electrolyte, where TiO$_2$ does not cover. The electron transfer from FTO to the external load is significantly faster than that of Eq. (6). Eq. (5) occurs more often than other ones because the concentration of I$_3^-$ is much higher than that of S$^+$. These recombination reactions

make the external current deteriorate and cause declines in voltage of DSSCs, which lead to low power conversion efficiency [10, 11].

Many efforts have been made for commercialization of DSSCs, including the investigation to enhance the efficiency and reduce the production cost of DSSCs, especially the research on cathodes and anodes. Various materials have been studied for the fabrication of electrodes in DSSCs: carbonaceous materials, conductive polymers, alloys, metal oxide, transition metal-based materials, etc. Among these materials, graphene is one of the most prospective materials for the synthesis of composites for fabrication of electrodes in DSSCs [14, 15].

3. Graphene for fabrication of electrodes in DSSCs

3.1 Carbonaceous materials

Carbon has long been an intriguing material because it had two allotropes which were widely known: diamond and graphite. Although these materials have the same elemental composition, the properties of graphite are very different from those of diamond. Although researchers working on carbon have long been aware of other forms, usually they were regarded as a nuisance and discarded if their formation could not be avoided. The importance of the recent "discoveries" of fullerenes and carbon nanotubes resides in the fact that their structures were elucidated for the first time. The most recent "discovery" is that of graphene, it is simply one of the many parallel sheets constituting graphite. The ingenuity resided in the preparation of a single isolated sheet, which opened the possibility of examining experimentally what was already a well-studied material theoretically [16].

Carbon-based materials have shown great versatility due to the ability to chemically combine with other carbon-based materials and with a range of different elements to form strong covalent bonds. As a result, these materials exhibit excellent characteristics such as high strength, high density, and high hardness. Their research, development and innovation are taking place in various fields, and studies employing the development of carbon-based materials have shown many positive results for a wide variety of structures, which has allowed the development of several materials with different applications [17].

Graphite is one of the most common allotropes of carbon, and the most stable form of carbon under standard conditions. Graphite is another promising electrode electrocatalyst and conducting layer material due to the abundant defect sites and good electronic properties. Particularly, the defect sites from edge planes are preferred to those of basal planes, as the former exhibits the faster electrons transport and charge transfer [18].
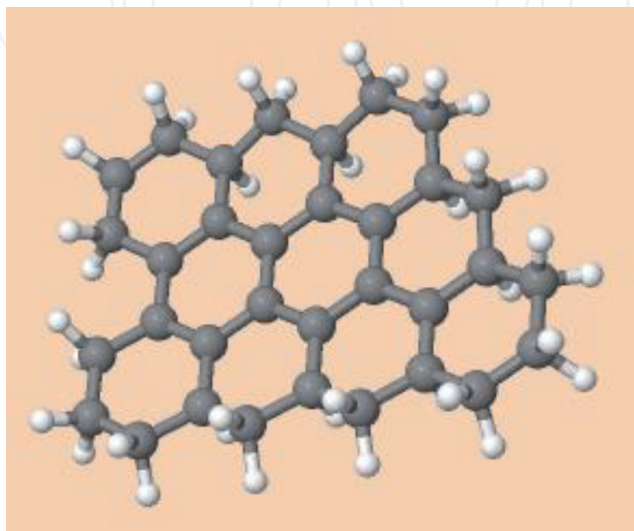
The three new materials, graphene, carbon nanotubes and fullerenes, can be called "nanocarbon" materials. Like graphite, the structures of these carbonaceous materials consist of sp^2 orbitals. Fullerenes contain 12 pentagons and have some sp^3 character. Fullerenes are spheroidal molecules and are made exclusively of carbon atoms (e.g. C60, C70). Their unique hollow cage-like shape and structural analogy with clathrin-coated vesicles in cells support the idea of the potential use of fullerenes as drug or gene delivery agents. Fullerenes display a diverse range of biological activity, which arises from their reactivity, due to the presence of double bonds and bending of sp^2 hybridized carbon atoms, which produces angle strain. Fullerenes can act either as acceptors or donors of electrons. When irradiated with ultraviolet or visible light, fullerenes can convert molecular oxygen into highly reactive singlet oxygen. Thus, fullerenes have the potential to inflict photodynamic damage on biological systems, including damage to cellular membranes, inhibition of various enzymes [18].

Carbon nanotubes (CNTs) are formed by a single cylindrically shaped graphene sheet called single-wall carbon nanotubes (SWCNTs) or several graphene sheets arranged concentrically called multi-wall carbon nanotubes (MWCNTs). CNTs have been proposed as the prospective substitutes for the conventional Pt in DSSCs due to their outstanding advantages of large surface area, high electrical conductivity, and chemical stability [18, 19]. Additionally, CNTs could also be used for synthesis of composite materials of anodes in DSSCs, including the ZnO nanowires/CNTs and TiO2/CNTs, in order to offer a potential platform to enhancement surface area and decrease of carrier recombination in DSSCs [20, 21].

As mentioned, carbonaceous materials are quite attractive for replacement of Pt in DSSCs due to the high electronic conductivity, corrosion resistance toward I_2 electrolyte, high reactivity for I_3^- reduction, and low cost. The lower catalytic activity of carbon compared to Pt can be compensated by increasing the active surface area of the electrode by using a porous electrode structure. For example, porous carbon electrodes are easily prepared from graphite powder, which consists of plate-like crystals that, on deposition from a liquid dispersion and drying, will preferentially align in the plane of the counter electrodes, resulting in a high conductivity in this plane. Numerous carbonaceous materials were studied for the fabrication of electrodes in DSSCs, using carbon vulcan, carbon black, activated carbon, carbon nanofibers, carbon nanotubes, graphene or the combination of these materials to fabricate the high-performance electrodes of DSSCs, like graphite-activated carbon [22], carbon black-graphite [23]. Among these materials, graphene has attracted the most attention of researchers due to its outstanding properties [5, 24].

3.2 Graphene

Andre Konstantin Geim and Konstantin Sergeevich Novoselov of the University of Manchester received the 2010 Nobel Prize in Physics for their pioneering research on graphene. Graphene is a flat monolayer of carbon atoms arranging like the structure of honeycombs with one atom thickness. Due to the special thickness, graphene is considered as a 2D material, as shown in **Figure 2**. Carbon atoms in graphene lattice are hybridized sp^2 with the C-C bond length of 1.42 Å. Graphene is one of the basic carbon allotropes, including graphite, carbon nanotube, and fullerene. Graphene possesses not only all properties of graphite but also other extraordinary characteristics. Graphene has high carrier mobility at room

Figure 2.
Structure of graphene.

temperature ($\sim$200,000 cm^2 V^{-1} s^{-1}), high specific area (2630 m^2 g^{-1}), excellent thermal conductivity ($\sim$3000 Wm^{-1} K^{-1}), high Young modulus ($\sim$1 TPa), and high optical transparency (97.7%). Moreover, although graphene has low-density, it is up to 50 times stronger than steel [24, 25].

Because graphene is an atom-thick layer, it is a perfect nanoscale material and, therefore, has great potential in a very wide range of applications in the field of nanotechnology. Graphene has been extensively studied for nano-technological applications in field-effect transistors, solar cells, fuel cells, supercapacitors, rechargeable batteries, optical modulators, chemical sensors, drug delivery, and biomedical applications, in addition to other areas [26, 27].

There are numerous methods for synthesis of graphene: mechanical exfoliation, chemical vapor deposition, epitaxial growth, chemical reduction, etc. [28, 29]. Among these methods, chemical reduction is a commonly used route for graphene synthesis. In this method, graphene is synthesized by reduction of graphene oxide (GO), which has the similar structure to graphene, with oxygen-containing functional groups introduced into the hexagon structure of graphene sheets. The synthesized graphene by this method is called rGO. Chemical reduction method is a cost-effective and widely available method for the mass production of rGO compared with thermal reduction and other methods. Otherwise, the synthesis procedure of graphene with bottom-up methods has revealed difficulty for applications in industry [30]. In this study, GO was synthesized from graphite (Gi) using the Hummers' method and GO was reduced to create rGO.

3.3 Graphene for fabrication of cathodes in DSSCs

In DSSCs, cathode carries out three functions. As a catalyst, the cathode facilitates the regeneration of redox couple i.e., the oxidized state of redox couple is reduced by accepting electrons at the surface of the electrode. As a positive electrode of primary cells, the cathode collects electrons from the external circuit and transfers electrons into the cell. As a mirror, unabsorbed light came through the photoanode and the electrolyte, which was partially reflected in the cell to enhance the utilization of the light [5, 31].
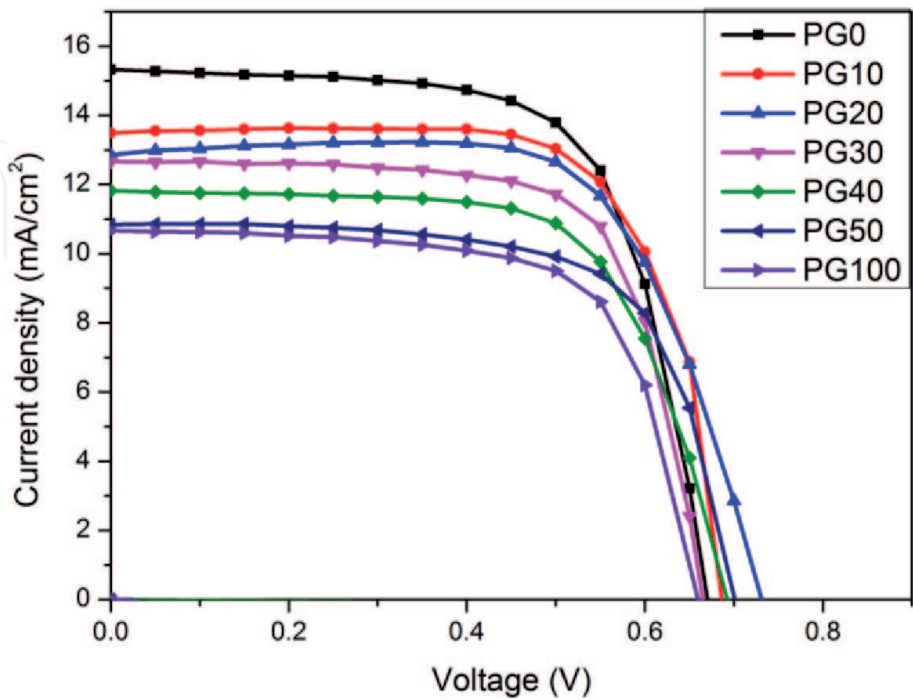
The cathode in DSSCs conventionally includes two parts: the substrate and the catalytic layer. The type of substrate mostly used in DSSCs is conductive glass substrates made by coating a layer of TCO on transparent glass. In DSSCs, the TCO substrate plays an important role in transmitting the incident light and leading the electrical current. Both transmittance and conductivity are crucial for the electrode of DSSCs. The conductive glass that is widely used in the fabrication of DSSCs is FTO [5].

For promoting the commercialization of DSSCs, the production cost of DSSCs needs to be reduced. Moreover, the efficiency of DSSCs is expected to maintain at an acceptable level. At present, Pt is still the most appropriate material for the fabrication of cathode in DSSCs. However, this noble metal has limited availability and relatively high cost that hinder the large-scale production of DSSCs. Moreover, Pt cathodes show poor resistance toward corrosion in iodide solution, which may result in the formation of PtI$_4$. The use of Pt in cathodes is considered as one of many reasons that prevent the commercialization of DSSCs. On the other hand, carbon is the material that can be found everywhere on the planet. Carbon-based materials had wide applications in technology including solar technology [5]. Recently, graphene has been explored as a novel material with many outstanding characteristics, which makes these materials become one of the most promising alternatives of Pt in DSSCs. In recent years, graphene and graphene-based materials have been demonstrated to be an adequate substitute for Pt, to cut off the use of

the noble metal and maintain the performance of DSSCs [32, 33]. Many research studies have been conducted to synthesized Pt/graphene or Pt/rGO with different methods. Yen et al. mixed GO and H_2PtCl_6 precursor salt in an ethylene glycol/H_2O mixture and heated the mixture at 120°C to form the Pt/rGO nanocomposite [34]. With the similar method, Khoa et al. mixed GO and H_2PtCl_6 with different amount of GO and then the mixture was heated at 350°C to obtain the Pt/thermally reduced graphene oxide composite [35]. Instead of thermal reduction method, Wan et al. used $NaBH_4$ as reducing agent for synthesis of Pt/rGO composite for cathode of DSSCs [36]. Recently, Yu et al. synthesized the Pt nanoparticles-loaded holey reduced graphene oxide framework materials with the addition of aqueous hydrofluoric acid, resulting in the high electrocatalytic activity and efficient electron/ion transport material for cathode fabrication of DSSCs [33]. After that, Suriani et al. combined graphene, SWCNT, and Pt to create the rGO/SWCNT hybrid film with low Pt loading for fabrication of cathode in DSSCs [37]. Beside these studies, there were various advanced methods for synthesis of Pt/graphene composite and other graphene-based materials: chemical vapor deposition [38, 39], hydrothermal, coating with different layers [40], etc. All of the fabricated DSSCs from mentioned studies exhibited high conversion efficiency that can be compared with DSSCs fabricated from the pure Pt cathodes.

Our group conducted the experiments to investigate the performance of Pt/rGO cathodes in DSSCs. Accordingly, rGO was synthesized from GO, which was synthesized from Gi using the improved Hummers' method. The Pt/rGO composite pastes were fabricated from rGO and H_2PtCl_6 with different weight percents of rGO: 0, 10, 20, 30, 40, 50, and 100 wt%, marked as PG0, PG10, PG20, PG30, PG40, PG50, and PG100, respectively. These composite pastes were used for fabrication of cathodes in DSSCs using the screen-printing technology. DSSCs were assembled with fabricated cathodes, Dyesol TiO2 anodes, N719 dye, and Dyesol High Stability Electrolyte (HSE). The efficiency of fabricated DSSCs was measured using the current density-voltage (J-V) curves. The J-V curves and the photovoltaic parameters of fabricated DSSCs are presented in **Figure 3** and **Table 1**.

Figure 3.
J-V curves of DSSCs fabricated from Pt/rGO cathodes with different weight percents of rGO. Reproduced with permission Ref. [32]. Copyright 2020, Elsevier.
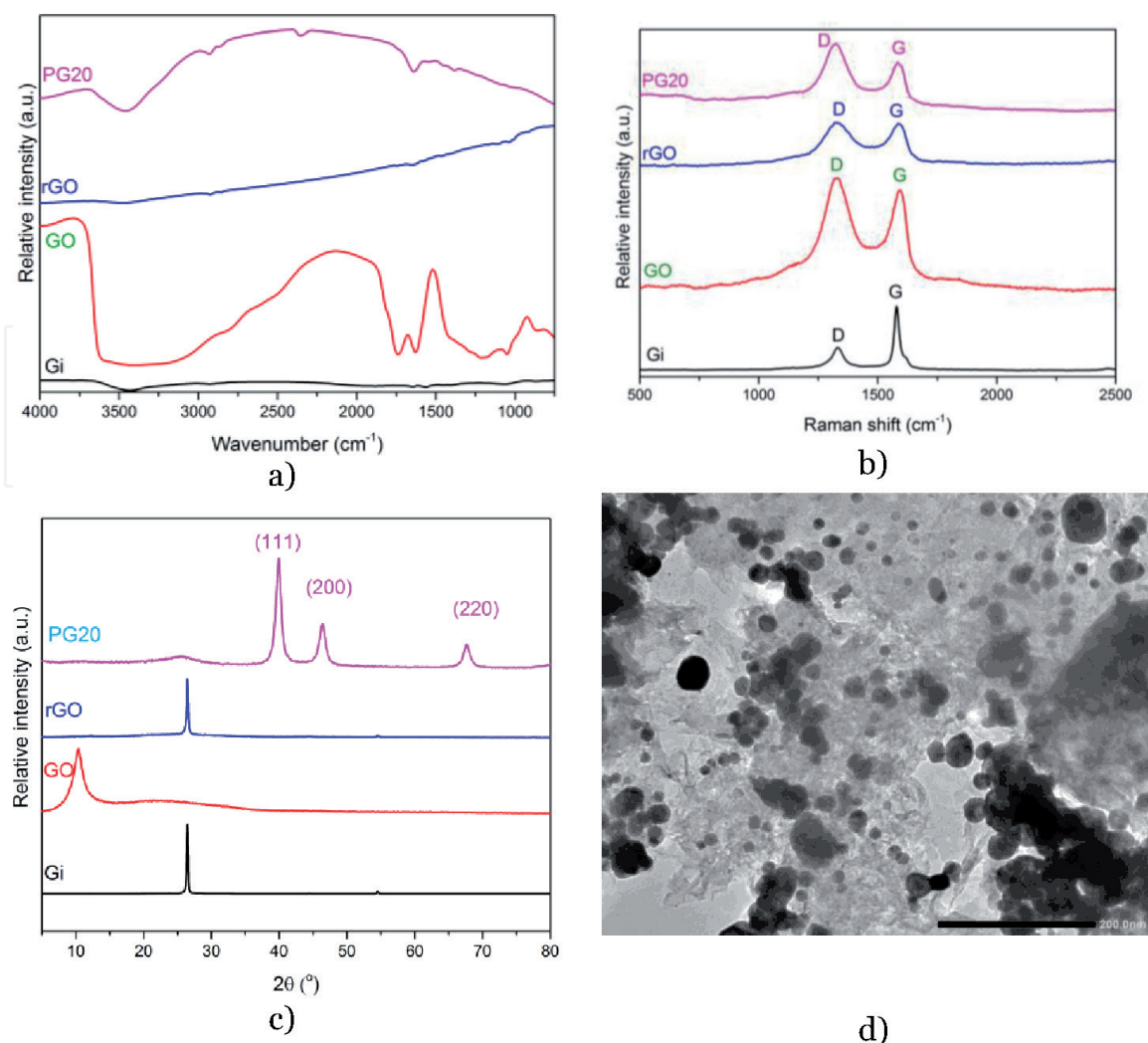
DSSCs	VOC (V)	J_{SC} (mA cm^{-2})	ff	η (%)
PG0	0.67	15.33	0.67	6.89
PG10	0.73	13.49	0.68	6.64
PG20	0.73	12.86	0.68	6.42
PG30	0.66	12.67	0.70	5.94
PG40	0.69	11.82	0.66	5.44
PG50	0.70	10.84	0.68	5.18
PG100	0.66	10.67	0.68	4.76

Table 1.
Photovoltaic parameters of DSSCs fabricated from Pt/rGO cathodes with different weight percents of rGO. Reproduced with permission Ref. [32]. Copyright 2020, Elsevier.

The J-V curve results showed that the conversion efficiency values of fabricated DSSCs was reduced when the amount of H_2PtCl_6 was reduced. In the structure of cathode, Pt nanoparticles played the catalytic and charge transferring roles. Since the intrinsic conductivity of rGO was relatively lower than that of Pt, the catalytic activities of Pt/rGO cathodes were lowered, leading to the decrease in efficiency [32]. However, rGO with the high surface area could play the role of supporting material to improve the electrochemical activity of Pt/rGO cathode. Therefore, Pt nanoparticles could be uniformly decorated on the surface of rGO lattice [41]. The high surface area of the Pt/rGO helps to maintain the high efficiencies of DSSCs in spite of the low conductivity of rGO, compared with Pt [42]. These results exhibited that the PG10 and PG20 DSSCs had better performance compared to other composite DSSCs, with efficiency values higher than 93% compared to PG0. The J-V results showed that PG20 was the appropriate material for fabrication of cathodes in DSSCs with high amount of Pt replacement and high conversion efficiency.

The Pt/rGO material in our study was investigated using different characterization technique like Fourier-transform infrared spectroscopy (FTIR), Raman spectroscopy, X-ray diffraction (XRD), and transmission electron microscopy (TEM). As shown in **Figure 4a**, the FTIR spectrum of GO revealed the vibrations peaks of the epoxide (C–O–C), alkene (C=C), and carboxyl functional groups (–COOH), at about 1050, 1628, and 1738 cm^{-1}, respectively. The broad peak at 3386 cm^{-1} originated from vibrations of hydroxyl (–OH) groups. The FTIR result demonstrated that during the oxidation process of Gi by improved Hummers' method, the oxygen-containing functional groups were introduced to the carbon framework of Gi to obtain GO [43]. For rGO, characteristic peaks could not be obviously determined, proving that the functional groups in the structure of GO were reduced. Similarly, the characteristic peaks of functional groups in the spectrum of PG20 were decreased, compared with GO, due to the functional groups remaining in the carbon lattice of PG20 after the reduction process [44].

As shown in **Figure 4b**, the Raman spectra of Gi, GO, rGO, and PG20 showed two characteristic peaks at around 1350 and 1580 cm^{-1}, corresponding to D and G-band peak. While G band relates to the vibration of sp^2 carbon network, the D band attributed to the structural defects and partial distortion in the structure of sp^2 carbon network. The ratios of D-band to G-band (I_D/I_G) represent the levels of defect in graphene-based materials [45]. The I_D/I_G value of GO is higher than that of Gi and lower than rGO or PG20, showing that the oxidation and reduction process increased the levels of defect in the structure of graphene sheets. The I_D/I_G value of PG20 was measured to be 1.12, where that of rGO accounts for 1.07.

Figure 4.
Characterization of PG20 and precursor materials: (a) FTIR spectra, (b) Raman spectra, (c) XRD patterns, and (d) TEM image. Reproduced with permission Ref. [32]. Copyright 2020, Elsevier.

This means that the level of defect in the structure of PG20 is higher than that of rGO, this was attributed to the incorporation of Pt nanoparticles into the rGO sheets [46].

The XRD patterns of Gi, GO, rGO, and PG20 are presented in **Figure 4c**. In the pattern of GO, there is a characteristic peak (002) at 2θ = 10.42°, corresponding to the interlayer distance of 0.85 nm. For rGO, the (002) peak appears at 2θ = 26.87°; the interlayer distance between the rGO sheets was determined to be 0.33 nm. The diffraction peak of GO pattern is not observed in the pattern of rGO, indicating the removal of functional groups of GO during the reduction process. In the pattern of PG20, the diffraction peaks are determined at 2θ = 39.97, 46.36, and 67.69 °, corresponding to the (111), (200), and (220) crystalline planes of Pt nanoparticles, respectively. Additionally, there is a diffraction peak at 2θ = 25.32° in the pattern of PG20, which was similar to that of rGO. The XRD result proved the formation of Pt particles from H_2PtCl_6 and the reduction of GO to create the rGO sheets, proving the successful synthesis of Pt/rGO [46].

The morphology of PG20 composite was investigated using the TEM images. As shown in **Figure 4d**, rGO is observed to be the semi-transparent thin layer, indicating that the 2D structure of rGO was maintained after the annealing process. The Pt nanoparticles are observed as the black spheres which were decorated on the rGO sheets. From the TEM images, the sizes of the Pt nanoparticles were estimated to be in range of 10–30 nm. Besides, the Pt nanoparticles were eventually decorated on the

rGO sheets. However, the Pt nanoparticles tended to agglomerate to form Pt clusters. The TEM images showed the high degree of agglomeration of Pt nanoparticles and the role of rGO as an effective supporting material in order to keep the distribution of Pt particles. The role as a supporting material of rGO helped to maintain the efficiency of PG20 DSSCs by increasing the surface areas of the materials.

The investigation of Pt/rGO cathodes in DSSCs proved that rGO was an excellent replacement for Pt in cathodes of DSSCs. By using the Pt/rGO composite for fabrication cathodes of DSSCs, the amount of Pt in DSSCs could be reduced and the efficiency could be maintained.

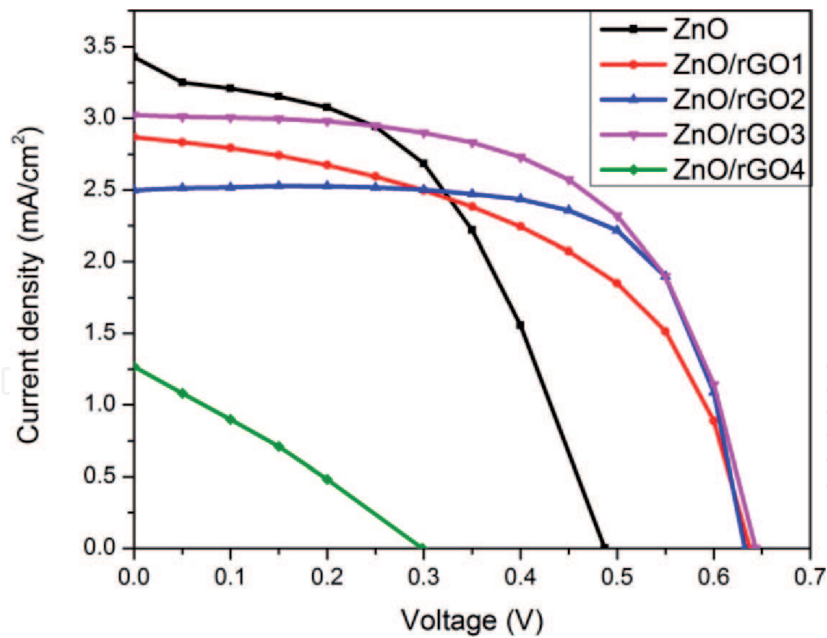### 3.4 Graphene for the fabrication of anodes in DSSCs

Three key factors that affect the DSSC efficiency have been extensively studied: photo-electron generation, charge carrier transfer, and surface reaction. The unique and outstanding properties of graphene are ideal for addressing these factors. Graphene offers a 2D conductive support path for electron transfer, which can improve the electron transfer in photoanode materials and reduce the electron-hole recombination rate. For an example of TiO_2, without carbonaceous material supporter, electrons that are injected into TiO_2 nanoparticles may transfer around and need a much longer transfer distance. Graphene provides a faster electron transfer path and significantly reduces the electron-hole recombination rate in the TiO_2 material layer. Additionally, the large surface area creates more occasions for reactive group decoration and enhances the chemical reaction and reduction processes [11, 47].

ZnO materials have been made into composite/hybrid materials along with other metallic as well as graphitic structures to enhance their mechanical and electrochemical properties [48]. ZnO has superior optical and electrical properties that include high electron mobility in the order of 1500 $cm^2 V^{-1} s^{-1}$ at room temperature, wide band gap energy of 3.3 eV, and a high excitation (electron-hole) binding energy of 60 meV. However, to overcome the drawback of poor catalytic activity in ZnO due to its photoelectron recombination, many studies had incorporated graphene into the ZnO matrix to its efficiency and reduce the electron recombination process [49, 50]. There are two main method for fabrication of ZnO/rGO composite: the in-situ method, which used the Zn(II) precursor salts and mixed with GO or rGO [51, 52], and the ex-situ method, which used the ZnO nanomaterials (nanoparticles, nano wires, nanorods, etc.) and mixed with rGO [53, 54].

Our group conducted the experiments to investigate the performance of ZnO/rGO anodes in DSSCs. Accordingly, ZnO/rGO composite materials were synthesized from $Zn(O_2CCH_2)_3$ and GO. The ZnO/rGO anodes were fabricated from ZnO/rGO composite materials with different weight percent of rGO: 0, 0.1, 0.5, 1, and 5 wt% corresponding to ZnO, ZnO/rGO1, ZnO/rGO2, ZnO/rGO3, and ZnO/rGO4, respectively. DSSCs were assembled with fabricated anodes, cathodes from Dyesol Platinum Paste, N719 dye, and HSE electrolyte. The efficiency values of fabricated DSSCs were measured using the J-V curves. The results showed that the DSSCs fabricated from ZnO/rGO anodes demonstrated the high efficiencies, compared with DSSCs using the ZnO anode. The J-V curves and the photovoltaic parameters of fabricated DSSCs are presented in **Figure 5** and **Table 2**.

As shown in **Figure 5**, the efficiencies of ZnO/rGO1, ZnO/rGO2, and ZnO/rGO3 DSSCs were determined to be 1.25, 1.47, and 1.55%, respectively, which were higher than that of ZnO DSSC (1.08%). During the transfer process of the excited electron from N719 to FTO, the electron-hole recombination could significantly deteriorate the performance of DSSCs, leading to the decrease in the conversion

Figure 5.
J-V curves of DSSCs fabricated from ZnO/rGO anodes with different weight percents of rGO. Reproduced with permission Ref. [50]. Copyright 2020, Chemical Engineering Transaction.
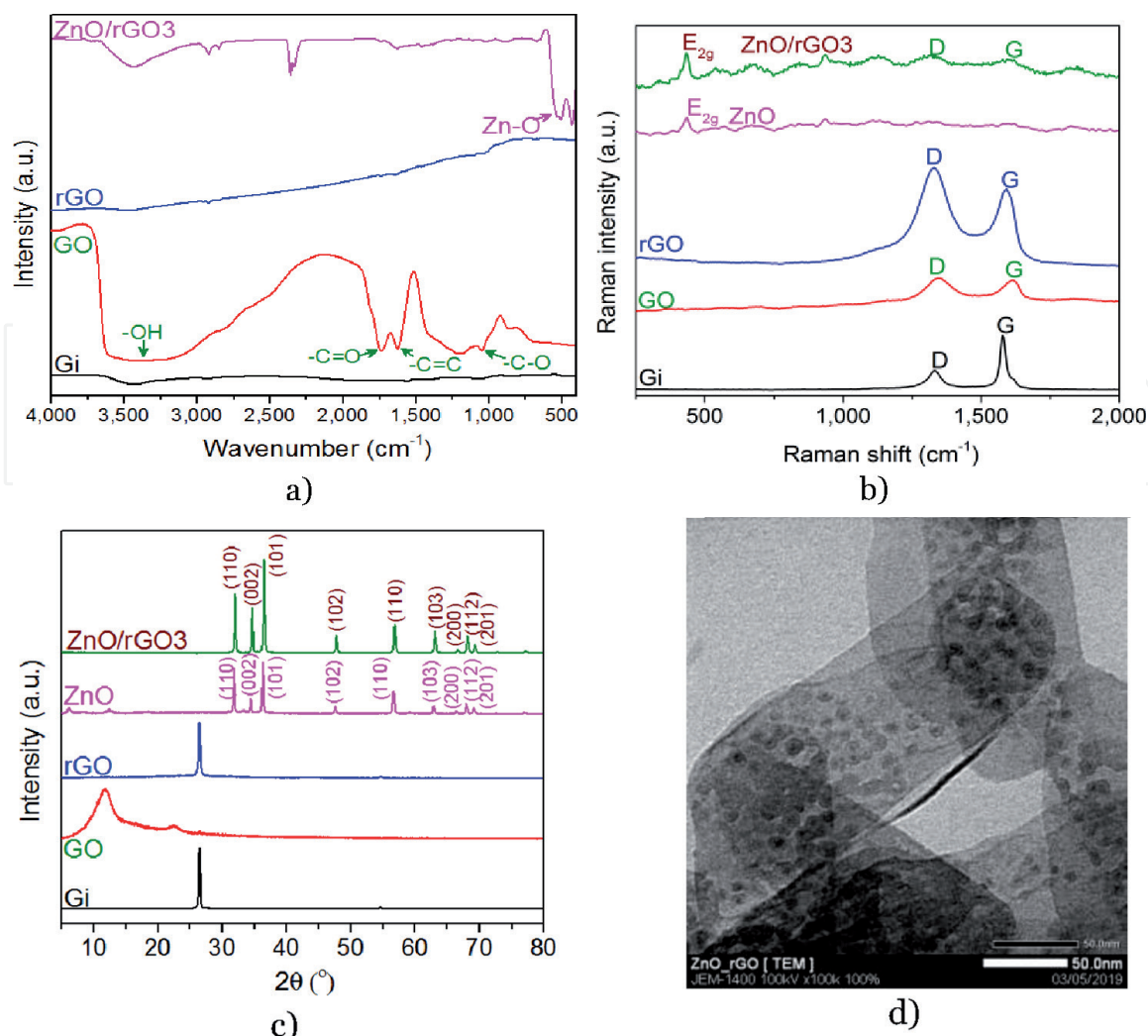
DSSCs	VOC (V)	J_{SC} (mA cm^{-2})	ff	η (%)
ZnO	0.48	3.43	0.49	1.08
ZnO/rGO1	0.64	2.87	0.51	1.25
ZnO/rGO2	0.63	2.50	0.70	1.47
ZnO/rGO3	0.64	3.02	0.60	1.55
ZnO/rGO4	0.30	1.27	0.28	0.14

Table 2.
Photovoltaic parameters of fabricated from ZnO/rGO anodes with different weight percents of rGO. Reproduced with permission Ref. [50] Copyright 2020, Chemical Engineering Transaction.

efficiency values. The addition of rGO, a material with high conductivity and high electron mobility, could improve the transfer pathway of the excited electron. The introduction of rGO in the structure of the anode material could help to prevent the recombination reactions and enhanced the efficiency of DSSC. ZnO/rGO4 DSSC demonstrated a low efficiency, because transmittance of anode was drastically decreased, due to the high amount of rGO in ZnO/rGO4 composite. Besides, the excessive amount of rGO could become the recombination center that increased the recombination reactions [55, 56]. Therefore, the appropriate rGO weight percent in the composite was 1%, corresponding to the ZnO/rGO3 DSSC.

The ZnO/rGO material in our study was characterized using various methods including: FTIR spectroscopy, Raman spectroscopy, XRD patterns, and TEM images. **Figure 6a** demonstrates the FTIR spectra of ZnO/rGO3 and precursor materials. As mentioned above, the FTIR results showed that Gi was oxidized to obtain GO. The characteristic peaks of GO were reduced or disappeared on the spectra of GO and ZnO/rGO, indicating that the functional group of GO was reduced to create rGO and ZnO/rGO. The FTIR spectrum of ZnO/rGO3 revealed two typical peaks at 507.14 and 433.23 cm^{-1}, corresponding to the Zn-O vibration of hexagonal wurtzite structure of ZnO [49].

As shown in **Figure 6b**, Raman spectra of ZnO/rGO3 and precursor materials had the D and G-band peak. In the Raman spectra of ZnO and ZnO/rGO3, the

Figure 6.
Characterization of ZnO/rGO3 and precursor materials: (a) FTIR spectra, (b) Raman spectra, (c) XRD patterns, and (d) TEM image. Reproduced with permission Ref. [50]. Copyright 2020, Chemical Engineering Transaction.

vibration peak at 436 cm^{-1} was assigned to the E$_2$ non-polar phonon modes, corresponding to the hexagonal crystal structure of ZnO nanoparticles. The D-band and G-band peaks of ZnO/rGO3 spectrum were unclear, due to the low amount of rGO in the structure of ZnO/rGO3 [57].

The XRD patterns of ZnO/rGO3 and precursor materials are demonstrated in **Figure 6c**. The characteristic diffraction peaks of ZnO/rGO3 were observed at 2θ = 31.8, 34.5, 36.3, 47.5, 56.6, 62.8, 67.9, and 69.0°, corresponding to the (110), (002), (101), (102), (110), (103), (112), and (201) crystalline plane of wurtzite structures; similar with the JCPDS File No.36-1451 of ZnO [55, 58]. The diffraction peaks of GO and rGO were not observed in the pattern of ZnO/rGO3, because the weight percent of rGO in ZnO/rGO3 composite was low (1%).

As shown in **Figure 6d**, the TEM images of the ZnO/rGO3 demonstrated the decoration of ZnO nanoparticles on rGO sheets. As mentioned above, rGO is observed to be the semi-transparent thin layer, while the ZnO nanoparticles are the black spheres. The average size of ZnO nanoparticles was estimated to be about 10 nm. As can be seen, the ZnO nanoparticles were evenly distributed on rGO sheets. These results exhibited the good incorporation of rGO sheets and ZnO nanoparticles in the structure of ZnO/rGO3.

The investigation of ZnO/rGO anodes in DSSCs proved that the incorporation of rGO into the structure of ZnO could enhance the efficiencies of DSSCs. Therefore, the ZnO/rGO composite is the appropriate material for the fabrication of anodes in DSSCs.

4. Conclusion

In this chapter, the use of graphene as a supporting material for electrodes in DSSCs was discussed. Graphene-based DSSCs have emerged as an important class of photovoltaic material for many recent years. Graphene could be synthesized by a chemical reduction method and called rGO. This chapter demonstrates that graphene (or rGO) is the prospective material for the synthesis of composite materials, including Pt/rGO and ZnO/rGO, which were applied for the fabrication of cathodes and anodes in DSSCs. Graphene has shown great potential to replace Pt as cathodes for fabricating DSSCs. The mentioned experiments of PG20 demonstrated that Pt nanoparticles supported on rGO could help to reduce the amount of Pt in cathodes of DSSCs, while the high efficiencies were maintained. For anodes, the incorporation of rGO in ZnO/rGO composites enhanced the efficiencies of DSSCs, by reducing the electron recombination processes in the structure of anodes in DSSCs.

Based on the reported results, it is clear that graphene materials will have wide and promising applications in DSSCs. Various graphene-based materials with distinct properties should be extensively studied before they are practically applied for producing DSSCs.

Conflict of interest

The authors declare no conflict of interest.

Author details

Nguyen Huu Hieu[1,2]

1 Key Laboratory of Chemical Engineering and Petroleum Processing (CEPP Lab), Ho Chi Minh City University of Technology (HCMUT), VNU-HCMC, Vietnam

2 Faculty of Chemical Engineering, HCMUT, VNU-HCMC, Vietnam

*Address all correspondence to: nhhieubk@hcmut.edu.vn

IntechOpen

References

[1] Pashaei B, Shahroosvand H. Molecularly engineered ruthenium polypyridyl complexes for using in dye-sensitized solar cell. Inorganic Chemistry Communications. 2020;**112**:107737. DOI: 10.1016/j. inoche.2019.107737

[2] Subramaniam K, Athanas AB, Kalaiyar S. Dual anchored ruthenium (II) sensitizer containing 4-nitro-phenylenediamine Schiff base ligand for dye sensitized solar cell application. Inorganic Chemistry Communications. 2019;**104**:88-92. DOI: 10.1016/j. inoche.2019.03.043

[3] Arjunan AT, Senthil TS. Dye sensitised solar cells. Materials Technology. 2013;**28**(1-2):9-14. DOI: 10.1179/1753555712Y.0000000040

[4] Ye M, Wen X, Wang M, Iocozzia J, Zhang N, Lin C, et al. Recent advances in dye-sensitized solar cells: From photoanodes, sensitizers and electrolytes to counter electrodes. Materials Today. 2015;**18**(3):155-162. DOI: 10.1016/j.cej.2016.07.001

[5] Chen M, Shao LL. Review on the recent progress of carbon counter electrodes for dye-sensitized solar cells. Chemical Engineering Journal. 2016;**304**:629-645. DOI: 10.1016/j. cej.2016.07.001

[6] Kumar S, Mahajan M, Singh R, Mahajan A. Silver nanoparticles anchored reduced graphene oxide for enhanced electrocatalytic activity towards methanol oxidation. Chemical Physics Letters. 2018;**693**:23-27. DOI: 10.1016/j.cplett.2018.01.003. DOI: 10.1016/j.cplett.2019.136797

[7] Cai L, Hou B, Shang Y, Xu L, Zhou B, Jiang X, et al. Synthesis of Fe3O4/graphene oxide/pristine graphene ternary composite and fabrication electrochemical sensor to detect dopamine and hydrogen peroxide. Chemical Physics Letters. 2019;**736**:136797. DOI: 10.1016/j. cplett.2019.136797

[8] Sun L, Li Y, Dan Y, Lu X, Li X, Wang F, et al. Self-assembled composite thin film counter electrode of cobalt sulfide/functionalized graphene for dye-sensitized solar cells. Thin Solid Films. 2019;**679**:8-14. DOI: 10.1016/j. tsf.2019.04.012

[9] Wei L, Wang P, Yang Y, Dong Y, Fan R, Song W, et al. Enhanced performance of dye sensitized solar cells by using a reduced graphene oxide/TiO2 blocking layer in the photoanode. Thin Solid Films. 2017;**639**:12-21. DOI: 10.1016/j.tsf.2017.08.011

[10] Gong J, Liang J, Sumathy K. Review on dye-sensitized solar cells (DSSCs): Fundamental concepts and. Renewable and Sustainable Energy Reviews. 2012;**16**(8):5848-5860. DOI: 10.1016/j. rser.2012.04.044

[11] Singh E, Nalwa HS. Graphene-based dye-sensitized solar cells: A review. Science of Advanced Materials. 2015;**7**(10):1863-1912. DOI: 10.1166/ sam.2015.2438

[12] Low FW, Lai CW. Recent developments of graphene-TiO2 composite nanomaterials as efficient photoelectrodes in dye-sensitized solar cells: A review. Renewable and Sustainable Energy Reviews. 2018;**82**:103-125. DOI: 10.1016/j. compositesb.2018.01.013

[13] Yeoh ME, Chan KY. Recent advances in photo-anode for dye-sensitized solar cells: A review. International Journal of Energy Research. 2017;**41**(15):2446-2467. DOI: 10.1002/er.3764

[14] Tasis D. Recent progress on the synthesis of graphene-based

nanostructures as counter electrodes in DSSCs based on iodine/iodide electrolytes. Catalysts. 2017;**7**(8):234. DOI: 10.3390/catal7080234

[15] Ngidi NP, Ollengo AM, Nyamori VO. Heteroatom-doped graphene and its application as a counter electrode in dye-sensitized solar cells. International Journal of Energy Research. 2019;**43**(5):1702-1734. DOI: 10.1002/er.4326

[16] Ramsden JJ. Carbon-based nanomaterials and devices. In: Nanotechnology. United Kingdom: Elsevier Inc; 2011. pp. 189-197. DOI: 10.1016/B978-0-08-096447-8.00009-0

[17] Santos MC, Maynart C, Aveiro LR, Paz EC, Pinheiro VS. Carbon-based materials: Recent advances, challenges, and perspectives. In: Reference Module in Materials Science and Materials Engineering. [book on the Internet]. Elsevier Inc. DOI: 10.1016/B978-0-12-803581-8.09262-6

[18] Slepička P, Hubáček T, Kolská Z, Trostová S, Kasálková N, et al. The properties and application of carbon nanostructures. In: F Y. Polymer Science. London: InTech; 2013. pp. 175-201. DOI: 10.5772/51062

[19] Chen H, Liu T, Ren J, He H, Cao Y, Wang N, et al. Synergistic carbon nanotube aerogel–Pt nanocomposites toward enhanced energy conversion in dye-sensitized solar cells. Journal of Materials Chemistry A. 2016;**4**(9):3238-3244. DOI: 10.1039/C5TA10185A

[20] Kilic B. Produce of carbon nanotube/ZnO nanowires hybrid photoelectrode for efficient dye-sensitized solar cells. Journal of Materials Science: Materials in Electronics. 2019;**30**(4):3482-3487. DOI: 10.1007/s10854-018-00624-y

[21] Kilic B, Turkdogan S, Astam A, Ozer OC, Asgin M, Cebeci H, et al.

Preparation of carbon nanotube/TiO2 mesoporous hybrid photoanode with iron pyrite (FeS2) thin films counter electrodes for dye-sensitized solar cell. Scientific Reports. 2016;**6**:27052. DOI: 10.1038/srep27052

[22] Sun KC, Memon AA, Arbab AA, Sahito IA, Kim MS, Yeo SY, et al. Electrocatalytic porous nanocomposite of graphite nanoplatelets anchored with exfoliated activated carbon filler as counter electrode for dye sensitized solar cells. Solar Energy. 2018;**167**:95-101. DOI: 10.1016/j.solener.2018.04.002

[23] Don MF, Ekanayake P, Nakajima H, Mahadi AH, Lim CM, Atod A. Acetylene carbon black-graphite composite as low-cost and efficient counter electrode for dye-sensitized solar cells (DSSCs). Ionics. 2019;**25**(11):5585-5593. DOI: 10.1007/s11581-019-03071-9

[24] Roy-Mayhew JD, Aksay IA. Graphene materials and their use in dye-sensitized solar cells. Chemical Reviews. 2014;**114**(12):6323-6348. DOI: 10.1021/cr400412a

[25] Mohan VB, Lau KT, Hui D, Bhattacharyya D. Graphene-based materials and their composites: A review on production, applications and product limitations. Composites Part B: Engineering. 2018;**142**:200-220. DOI: 10.1016/j.compositesb.2018.01.013

[26] Zhu Y, Murali S, Cai W, Li X, Suk JW, Potts JR, et al. Graphene and graphene oxide: Synthesis, properties, and applications. Advanced Materials. 2010;**22**(35):3906-3924. DOI: 10.1002/adma.201001068

[27] Avouris P, Dimitrakopoulos C. Graphene: Synthesis and applications. Materials Today. 2012;**15**(3):86-97. DOI: 10.1016/S1369-7021(12)70044-5

[28] Lee HC, Liu WW, Chai SP, Mohamed AR, Aziz A, Khe CS, et al. Review of the synthesis, transfer,

characterization and growth mechanisms of single and multilayer graphene. RSC Advances. 2017;**7**(26):15644-15693

[29] Sattar T. Current review on synthesis, composites and multifunctional properties of graphene. Topics in Current Chemistry. 2019;**377**(2):10. DOI: 10.1007/ s41061-019-0235-6

[30] Smith AT, LaChance AM, Zeng S, Liu B, Sun L. Synthesis, properties, and applications of graphene oxide/ reduced graphene oxide and their nanocomposites. Nano Materials Science. 2019;**1**(1):31-47. DOI: 10.1016/j. nanoms.2019.02.004

[31] Samantaray MR, Mondal AK, Murugadoss G, Pitchaimuthu S, Das S, Bahru R, et al. Synergetic effects of hybrid carbon nanostructured counter electrodes for dye-sensitized solar cells: A review. Materials. 2020;**13**(12):2779. DOI: 10.3390/ma13122779

[32] Cuong LV, Thinh ND, Nghia LTT, Khoa ND, Hung LK, Dat HH, et al. Synthesis of platinum/reduced graphene oxide composite pastes for fabrication of cathodes in dye-sensitized solar cells with screen-printing technology. Inorganic Chemistry Communications. 2020;**118**:108033. DOI: 10.1016/j.inoche.2020.108033

[33] Yu M, Wu X, Zhang J, Meng Y, Ma Y, Liu J, et al. Platinum nanoparticles-loaded holey reduced graphene oxide framework as freestanding counter electrodes of dye sensitized solar cells and methanol oxidation catalysts. Electrochimica Acta. 2017;**258**:485-494. DOI: 10.1016/j.electacta.2017.11.086

[34] Yen MY, Teng CC, Hsiao MC, Liu PI, Chuang WP, Ma CCM, et al. Platinum nanoparticles/graphene composite catalyst as a novel composite counter electrode for high performance dye-sensitized solar

cells. Journal of Materials Chemistry. 2011;**21**(34):12880-12888. DOI: 10.1039/ C1JM11850A

[35] Khoa NT, Van Thuan D, Kim SW, Park S, Van Tam T, Choi WM, et al. Facile fabrication of thermally reduced graphene oxide–platinum nanohybrids and their application in catalytic reduction and dye-sensitized solar cells. RSC Advances. 2016;**6**(2):1535-1541. DOI: 10.1039/C5RA21896A

[36] Wan L, Luo T, Wang S, Wang X, Guo Z, Xiong H, et al. Pt/graphene nanocomposites with low Pt-loadings: Synthesis through one-and two-step chemical reduction methods and their use as promising counter electrodes for DSSCs. Composites Science and Technology. 2015;**113**:46-53. DOI: 10.1016/j.compscitech.2015.03.015

[37] Suriani AB, Mohamed A, Othman MHD, Mamat MH, Hashim N, Ahmad MK, et al. Reduced graphene oxide-multiwalled carbon nanotubes hybrid film with low Pt loading as counter electrode for improved photovoltaic performance of dye-sensitised solar cells. Journal of Materials Science: Materials in Electronics. 2018;**29**(13):10723-10743. DOI: 10.1007/s10854-018-9139-4

[38] Capasso ABS, Palma AL, Najafi L, Castillo AEDR, Curreli N, Pellegrini V. CVD-graphene/graphene flakes dual-films as advanced DSSC counter electrodes. 2D Materials. 2019;**6**(3):035007. DOI: 10.1088/2053-1583/ab117e

[39] Cheng CE, Lin CY, Shan CH, Tsai SY, Lin KW, Chang CS, et al. Platinum-graphene counter electrodes for dye-sensitized solar cells. Journal of Applied Physics. 2013;**114**(1):014503. DOI: 10.1063/1.4812498

[40] Lin CA, Lee CP, Ho ST, W TC, Chi YW, Huang KP, et al. Nitrogen-doped Graphene/platinum counter

electrodes for dye-sensitized solar cells. ACS Photonics. 2014;**1**(12):1264-1269. DOI: 10.1021/ph500219r

[41] Shih PT, Dong RX, Shen SY, Vittal R, Lin JJ, Ho KC. Transparent graphene–platinum nanohybrid films for counter electrodes in high efficiency dye-sensitized solar cells. Journal of Materials Chemistry A. 2014;**2**(23):8742-8748. DOI: 10.1039/C3TA12931D

[42] Wan L, Zhang Q, Wang S, Wang X, Guo Z, Dong B, et al. A two-step reduction method for synthesizing graphene nanocomposites with a low loading of well-dispersed platinum nanoparticles for use as counter electrodes in dye-sensitized solar cells. Journal of Materials Science. 2015;**50**(12):4412-4421. DOI: 10.1007/s10853-015-8998-9

[43] Chen W, Yan L, Bangal PR. Chemical reduction of graphene oxide to graphene by sulfur-containing compounds. The Journal of Physical Chemistry C. 2010;**114**:19885-19890. DOI: 10.1021/jp107131v

[44] Kempegowda R, Antony D, Malingappa P. Graphene–platinum nanocomposite as a sensitive and selective voltammetric sensor for trace level arsenic quantification. International Journal of Smart and Nano Materials. 2014;**5**(1):17-32. DOI: 10.1080/19475411.2014.898710

[45] Yang M, Zhao X, Yao C, Kong Y, Ma L, Shen X. Nanostructured cation disordered Li2FeTiO4/graphene composite as high capacity cathode for lithium-ion batteries. Materials Technology. 2016;**31**(9):537-543. DOI: 10.1080/10667857.2016.1192372

[46] Qiao J, Zhang L, Gao S, Li N. Facile fabrication of graphene-supported Pt electrochemical sensor for determination of caffeine. Applied Biochemistry and Biotechnology.

2020;**190**(2):529-539. DOI: 10.1007/s12010-019-03104-z

[47] Guo X, Lu G, Chen J. Graphene-based materials for photoanodes in dye-sensitized solar cells. Frontiers in Energy Research. 2015;**3**:50. DOI: 10.3389/fenrg.2015.00050

[48] Vittal R, Ho KC. Zinc oxide based dye-sensitized solar cells: A review. Renewable and Sustainable Energy Reviews. 2017;**70**:920-935. DOI: 10.1016/j.rser.2016.11.273

[49] Philip MR, Nguyen H, Babu R, Krishnakumar V, Bui TH. Polyol synthesis of zinc oxide-graphene composites: Enhanced dye-sensitized solar cell efficiency. Current Nanomaterials. 2018;**31**(5):52-60. DOI: 10.2174/2405461503666180507124310

[50] Nghia LTT, Phat LT, NTT M, Dat HH, Hung LK, Hien TM, et al. Synthesis of zinc oxide/reduced graphene oxide composites for fabrication of anodes in dye-sensitized solar cells. Chemical Engineering Transactions. 2019;**78**:61-66. DOI: 10.3303/CET2078011. DOI: 10.3303/CET2078011

[51] Jayabal P, Gayathri S, Sasirekha V, Mayandi J. Preparation and characterization of ZnO/graphene nanocomposite for improved photovoltaic performance. Journal of Nanoparticle Research. 2014;**16**(11):2640. DOI: 10.1007/s11051-014-2640-7

[52] Abdullah H, Atiqah NA, Omar A, Asshaari I, Mahalingam S, Razali Z, et al. Structural, morphological, electrical and electron transport studies in ZnO–rGO (wt%= 0.01, 0.05 and 0.1) based dye-sensitized solar cell. Journal of Materials Science: Materials in Electronics. 2015;**26**(4):2263-2270. DOI: 10.1007/s10854-015-2679-y

[53] Song JL, Wang X. Effect of incorporation of reduced graphene

oxide on ZnO-based dye-sensitized solar cells. Physica E: Low-Dimensional Systems and Nanostructures. 2016;**81**:14-18. DOI: 10.1016/j. physe.2016.02.005

[54] Chang WC. Graphene/ZnO nanoparticle composite photoelectrodes for dye-sensitized solar cells with enhanced photovoltaic performance. Journal of Nanoscience and Nanotechnology. 2016;**16**(9):9160-9165. DOI: 10.1166/jnn.2016.12900

[55] Bykkam S, Kalagadda VR, Kalagadda B, Selvam KP, Hayashi Y. Ultrasonic-assisted synthesis of ZnO nano particles decked with few layered graphene nanocomposite as photoanode in dye-sensitized solar cell. Journal of Materials Science: Materials in Electronics. 2017;**28**(8):6217-6225. DOI: 10.1007/s10854-016-6301-8. DOI: 10.1007/s10854-016-6301-8

[56] Siwach B, Mohan D, Jyoti D. To investigate opulence of graphene in ZnO/graphene nanocomposites based dye sensitized solar cells. Journal of Materials Science: Materials in Electronics. 2017;**28**(15):11500-11508. DOI: 10.1007/s10854-017-6946-y

[57] Khurana G, Sahoo S, Barik SK, Katiyar RS. Improved photovoltaic performance of dye sensitized solar cell using ZnO–graphene nano-composites. Journal of Alloys and Compounds. 2013;**578**:257-260. DOI: 10.1016/j. jallcom.2013.05.080. DOI: 10.1016/j. jallcom.2013.05.080

[58] Siwach B, Mohan D, Singh KK, Kumar A, Barala M. Effect of carbonaceous counter electrodes on the performance of ZnO-graphene nanocomposites based dye sensitized solar cells. Ceramics International. 2018;**44**(17):21120-21126